Integrating machine learning with rock physics for multizone property prediction

Paritosh Bhatnagar[1] and Anastasya Teitel[2]

https://doi.org/10.1190/tle-2025-1062

Abstract

Selecting appropriate rock physics models in geologically complex settings with limited core or lab measurements poses a significant challenge for reliable calibration and property prediction. This is further hindered in reservoirs with multiple stacked pay zones and varying depositional environments, where separate rock physics models (RPMs) are typically required for different rock types to ensure accurate log prediction. This study presentend a rock physics-guided machine learning workflow that integrated statistical learning with physically constrained rock physics models to predict facies, elastic, and petrophysical properties across multiple wells simultaneously. The method applied an expectation–maximization (EM) algorithm within a maximum-likelihood framework in which facies probabilities and RPM fitting parameters were jointly updated while remaining constrained within physically realistic bounds. This enabled automatic calibration of rock physics templates while simultaneously generating facies classifications and log predictions. The workflow was tested in two geologically distinct settings: the Athabasca Oil Sands in northeastern Alberta and the Barnett interval of the Midland Basin. Using common well-log inputs (gamma ray, density, neutron porosity, resistivity, and elastic logs where available), the workflow calibrated rock physics models for multiple facies and generated consistent elastic and petrophysical predictions across wells. Results from training and blind wells demonstrated that the method could reconstruct missing log suites, estimate elastic and petrophysical properties from limited inputs, and generate per-facies depth trends consistent with regional geology. The workflow not only streamlined RPM calibration but also supported reservoir characterization workflows, such as log repair, well-to-seismic ties, and construction of low-frequency models for seismic inversion, thereby enabling faster and more reliable interpretation in data-scarce environments.

Introduction

Calibrating rock physics models and predicting consistent elastic and petrophysical properties across multiple facies and wells remains challenging in data-scarce environments, particularly where conventional workflows such as rock physics calibration are manual and purely data-driven machine learning methods lack geologic and physical constraints. In recent years, the oil and gas industry has witnessed significant advancements in the application of machine learning (ML) and deep learning (DL), aiding in workflow efficiency and decision-making across exploration, development, and production. In the context of quantitative interpretation, common workflows include elastic and geomechanical log predictions (Suleymanov et al., 2023; Zhao et al., 2024; Liu et al., 2025), petrophysical modeling (Pandey et al., 2020), facies classification, and RPM calibration (Bianco, Bhatnagar, and Anantharamu, 2024), along with data-driven ML approaches (Verma et al., 2021; Anantharamu, Bhatnagar, and Bianco, 2024) that provide valuable insights for field development and reservoir trend mapping. However, many machine learning approaches rely primarily on statistical modeling and do not explicitly incorporate rock physics frameworks that constrain the relationships between elastic and petrophysical properties. Models trained on a specific field or stratigraphic setting often do not transfer well to another setting as geology varies. As new wells come online or geology becomes better understood, models may become outdated, requiring retraining and recalibration. If not guided by geologic constraints, ML can produce nonphysical logs, unrealistic facies transition, and depth trends that violate stratigraphy. Therefore, predicting complete suites of logs within a rock physics framework is advantageous for reservoir characterization workflows and, in turn, accurate property prediction within zones of interest.

Rock physics machine learning (RPML) uses rock physics principles to guide the ML models to stay within physical bounds and domain knowledge that pure data-driven models often miss. Rock physics-guided machine learning models enhance feature engineering (impedance contrast, elastic moduli, porosity transform, and rock physics-based facies templates) to improve model discrimination between facies and petrophysical properties. In some cases, rock physics forward modeling can predict logs for underrepresented facies or missing wells, which can help solve class imbalance issues and improve DL/ML training.

This study applies the RPML workflow in two areas, Athabasca Oil Sands in northeastern Alberta and the western margin of the Midland Basin (a subbasin in the greater Permian Basin, Figure 1).

The Athabasca oil sands in northeastern Alberta, Canada, provide an ideal setting to demonstrate RPML's application in a geologically complex heavy-oil system. Bitumen occurs primarily within the Cretaceous McMurray Formation, where highly porous fluvial channel sands are interlayered with muddy, clay-rich deposits that can impede or restrict steam and fluid

Manuscript received 14 December 2025; revision received 20 March 2026; accepted 9 April 2026; published ahead of production 23 April 2026.
[1]Ikon Science, Houston, Texas, USA. E-mail: pbhatnagar@ikonscience.com.
[2]Ikon Science, Calgary, Alberta, Canada. E-mail: ateitel@ikonscience.com.

movement (Leckie and Smith, 1992; Smith, 1994). These internal variations necessitate accurate facies models, which must remain geologically realistic to effectively guide in situ recovery strategies, such as steam-assisted gravity drainage (SAGD) (Smith and Lee, 2021).

In contrast, the stratigraphic framework of the Midland Basin reflects a complex interplay of depositional processes that produced heterogeneous successions of detrital limestones, siltstones, mudstones, calcareous, and organic-rich shales. Structural complexity and sediment supply from adjacent carbonate platforms further influenced sedimentation, resulting in distinctive facies architectures and spatial variability across the basin (Bhatnagar et al., 2019; Bhatnagar, Anantharamu, and Bianco, 2023). Of particular interest are low clay organic-rich shales within the Barnett interval, with high porosity and total organic carbon (TOC) that are potential targets for fracture simulation. There has been a recent resurgence of play where operators have tested the Barnett and Woodford benches. Wells drilled within the lower Barnett have shown promising results with expected ultimate recoveries (EUR) exceeding 1 million barrels of oil and 1.8 billion cubic feet (BCF) of gas (Lewis et al., 2024).

Depending on the location within these study areas, some of the facies can be drilling hazards, whereas others can act as a primary source for hydrocarbon generation. Therefore, accurately predicting elastic and petrophysical properties is key to successful reservoir characterization. The application of rock physics-based machine learning provides a framework for addressing these challenges in data-scarce environments and provides insights to target the right facies for fracture stimulation.

Methodology

RPML is a physics-constrained statistical learning workflow that integrates rock physics models with probabilistic modeling to estimate facies and predict reservoir properties. Each facies is associated with a selected rock physics model whose parameterization defines the expected relationship between elastic and petrophysical properties. An expectation–maximization (EM) optimization procedure is used to estimate facies probabilities and update model parameters while maintaining rock physics consistency in a multiwell setting. Using rock physics principles, the workflow focuses on the relationship between subsurface properties, such as porosity, saturation, mineralogy, and compaction effect. Templates from a pre-established rock physics model library are autocalibrated to the data, where the RPMs are checked for model relevancy and help improve accuracy for facies and log interpretation.

The process begins by defining a statistical model for each rock type using a multivariate Gaussian distribution whose mean varies with depth. These depth-dependent means are determined by the rock physics model (RPM) parameters and capture how rock properties change with depth. The variability around each rock type trend is described by a covariance matrix, which is assumed to remain constant with depth as well (Figure 2).

RPML takes advantage of the EM algorithm, a well-established iterative optimization technique for estimating maximum-likelihood parameters in statistical models, particularly when the data include hidden variables or are incomplete (Dempster, Laird, and Rubin, 1977). In this implementation, EM is used with strong spatial coupling to link each facies to a specific RPM, each characterized by a unique set of fitting parameters constrained to physically realistic ranges. These parameters are estimated through bound-constrained optimization embedded within the EM process. It is these model parameters, such as porosity, saturation, mineralogy, and compaction effect, that the rock physics models use to constrain the statistical model. Facies and RPM parameterizations are inferred from well-log data within the object framework of a maximum-likelihood approach, explicitly accounting for compaction and depth effects.

Wells with associated pressure trend, elastic, and petrophysical logs are combined with prior models, their fitting parameters, and prior proportions as inputs to the workflow. Each prior model includes an inherent fluid type (brine, oil, gas) and rock type (sand, shale, carbonate) that contain one or more mineral-related parameter groups. For a fitting parameter within a specific RPM, all related mineral moduli and petrophysical prior parameters are tied to the mineral mixer; RPML then solves for the mineral fraction that best fits the prior data, adjusting these parameters accordingly. RPML further relies on several hyperparameters that control the behavior and convergence of the EM algorithm, such

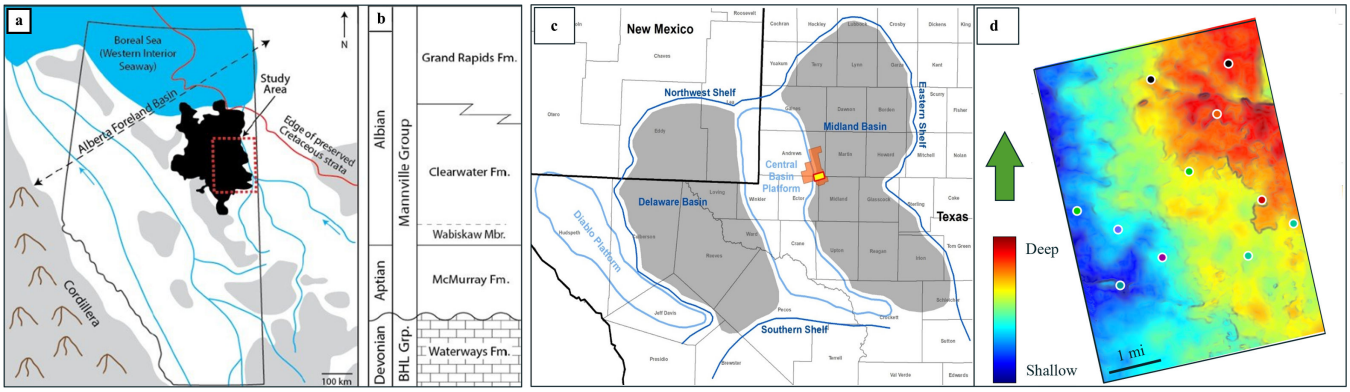

Figure 1. Overview of the study area and regional geologic framework. (a) Generalized Early Cretaceous paleogeography (reproduced with permission from **Leckie and Smith, 1992**). Areas interpreted as paleotopographic highs are shown in gray. The Athabasca oil sands region is shown in black. (b) Stratigraphic framework for the Mannville Group in northeastern Alberta. (c) Study area in the Midland Basin and (d) Early Pennsylvanian structure map showing wells used in the study area.

as damping factor, seeding, number of iterations, and outlier detection.

Once configured, RPML produces the final distribution parameters and assigns class memberships, resulting in a refined log prediction, facies classification, and calibrated RPMs across all rock types (Table 1). This provides a head start in creating RPM templates, which can then be shared easily among teams and represent the base start for further refined calibration.

Results and discussion

The methodology described was implemented in two onshore plays, although the workflow can be used in most conventional and unconventional settings for trend analysis, data repair, and facies classification. Inputs for the training included gamma ray (GR), photoelectric (PE), neutron porosity (CNL), resistivity (Resis), velocities (V_P, V_S), and density (Rho) logs. As with any ML-based application, it was ensured that input data were corrected for any inconsistencies such as missing gaps, tool-related errors, and processing issues. The RPML approach was then used to automatically classify facies using prior geologic knowledge of the region and a comprehensive library of rock physics models.

Northeastern Alberta. For Athabasca, three main facies were identified based on subsurface characteristics: oil sands, shaly sand, and shale. The oil sands facies are characterized by high porosity and permeability, typically containing bitumen and sand. The shaly sand, on the other hand, consists of a mixture of sand and clay with varying clay content, leading to intermediate porosity and permeability. These intervals are crucial for understanding transitional zones between oil sands and shale and can significantly impact fluid flow and reservoir characterization. The shale facies, characterized by a volume of shale above 70%, are composed predominantly of clay minerals. These intervals exhibit low permeability and are made up of fine-grained sedimentary rocks that act as key sealing units and barriers for fluid migration.

The Vernik and Kachanov (2010) sandstone model was selected as a practical framework for representing the observed velocity–porosity trends in the oil sand intervals. This model was chosen as it provided a convenient parameterization for representing elastic trends associated with variations in porosity and consolidation state. Although other formulations, such as Xu and Payne (2009) or Zhu et al. (2011), may also provide acceptable fits depending on the data set and calibration objectives.

For shaly sand intervals, the Vernik conventional shale model was used due to its flexibility in handling variations in nonclay minerals and clay content. This model provided a good fit for heterogeneous shaly sand and elastic property predictions by accounting for their mixed mineralogy and pore structure (Vernik and Kachanov, 2010; Vernik, 2016).

Shale intervals were modeled using the silty shale model, a simplified isotropic version of the anisotropic shale model by Pervukhina et al. (2015). It effectively captures shale bulk properties by incorporating porosity and clay variations, computing wet clay moduli using the lower Hashin–Shtrikman bound and averaging nonsilt moduli across the porosity range using both Hashin–Shtrikman bounds.

After going through several iterations in the EM algorithm, RPML picked the optimized value for each model parameter to produce facies distributions consistent with geologic

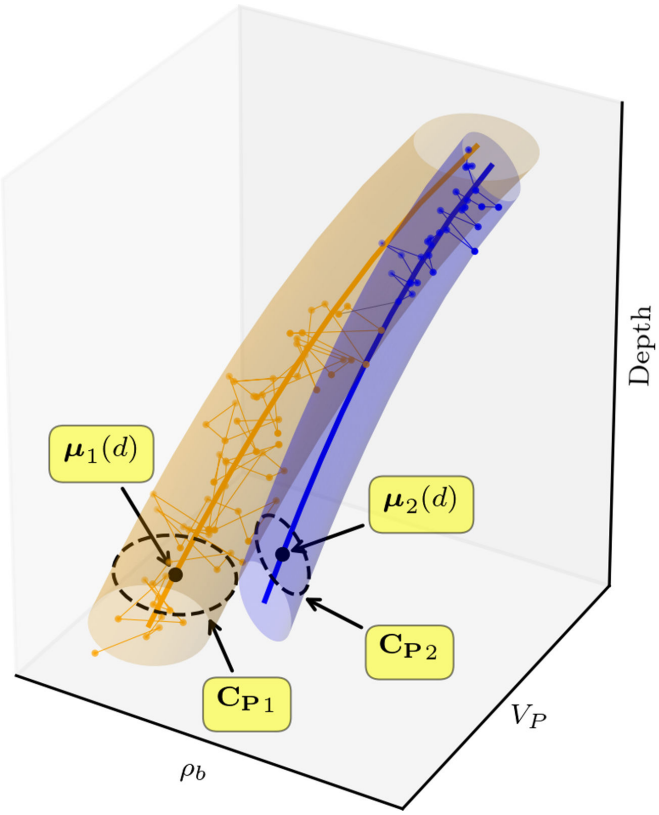

Figure 2. A schematic representation of the statistical framework used in the RPML process. Each rock type is modeled as a multivariate Gaussian distribution whose mean varies with depth along each dimension. This formulation captures geologic variability and enables facies classification by linking rock types to depth-dependent rock physics trends. μ is the facies-specific mean, and σ is the facies-specific variance for each property.

Table 1. Overview of the inputs needed for the RPML workflow, the variables estimated during the process and outputs generated across various rock types.

Inputs	Estimated Variables	Outputs
• Well logs: GR, PE, resistivity, neutron porosity, V_P, V_S, or ρ • Facies or lithology priors • Selected rock physics models • Parameter bounds for RPM calibration	• Model properties such as grain parameters (GR, CNL, PEF), porosity, resistivity, saturation, and mineralogy • Facies probabilities • Rock physics model relevancy	• Predicted petrophysical and elastic logs • Facies classification • Calibrated rock physics models • Posterior facies distribution

expectations, separating potential bitumen-bearing channel sands from transitional and sealing intervals at the log scale. Figure 3a highlights a representative well, illustrating the comparison between measured and RPML modeled log data, and the corresponding facies interpretation. The agreement between original and synthetic logs across the facies units supports the reliability of the model-based classification. RPML's ability to generate facies likelihood curves provides important context for understanding uncertainty and recognizing intervals where mixed or transitional lithologies may impact fluid flow. These intervals are particularly important for SAGD, as they can create subtle flow restrictions or preferential pathways that are not apparent from simple cut-off-based facies schemes. Also shown are per-facies depth trends (Figure 3b) that highlight RPML's prediction overlaid on the well data and understanding each facies elastic behavior due to any compaction or diagenesis effect.

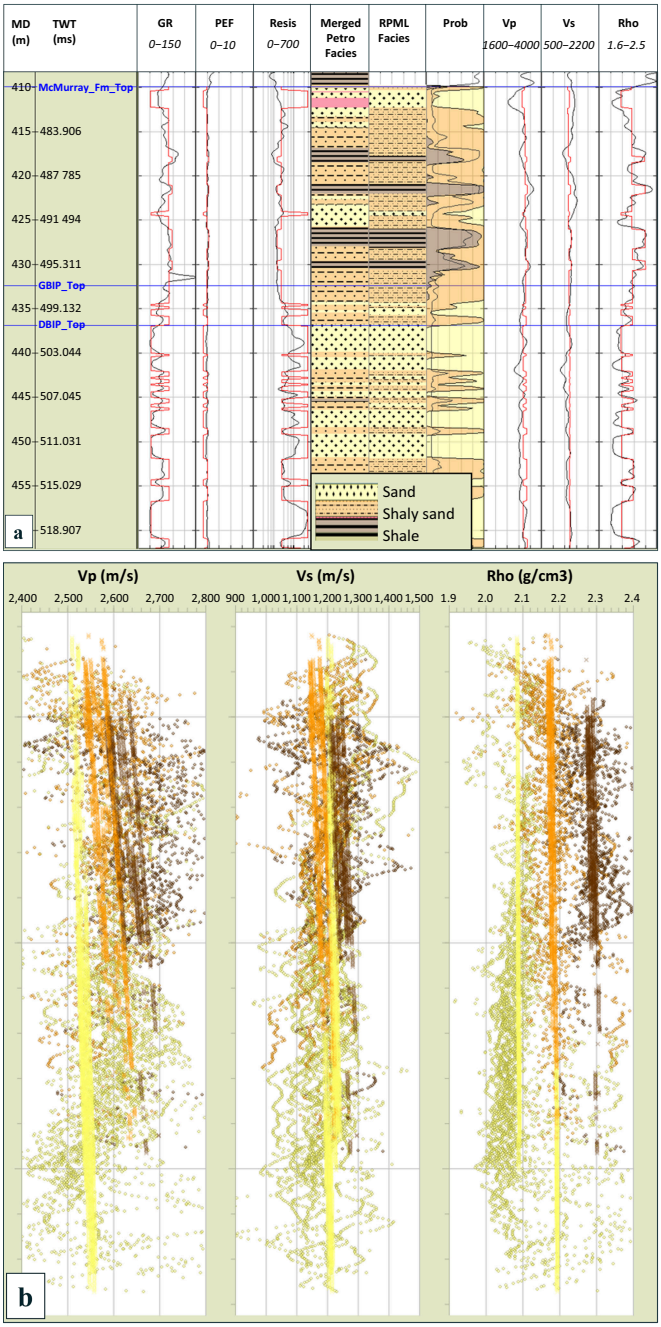

Figure 3. (a) Comparison between the original input logs (black curves) and the modeled logs (red curves) for a selected well from the study area. (b) Facies depth trend plots for oil sands, shaly sand and shale end members in Vp, Vs and Rho domain (Taken from: Teitel, 2025).

For additional quality control (QC), elastic property crossplots with the autofitted rock physics models were generated (Figure 4) to visually compare the observed log data with the theoretical model trends. The alignment and clustering of data points along the model curves indicate strong agreement between measured and predicted behavior, supporting the classification results and the suitability of the selected rock physics models for this study area.

Midland Basin. For this study area, RPML was applied within the Barnett interval to help characterize the varying clay content as well as predict facies that can pose as drilling hazards during well operations. The Midland Basin example demonstrates the applicability of the RPML workflow in a different geologic setting characterized by organic-rich shale and variable mineral composition. By applying the same workflow to sandstone-dominated and shale-dominated systems, the study illustrates the flexibility of the approach for multifacies reservoir characterization.

Vernik–Kachanov carbonate and Vernik conventional shale models were used for RPM fitting and model calibration. The Vernik Kachanov carbonate model is an extension of the sandstone model where the pore shape factor is porosity-related, and the crack density parameter is effective stress-related due to gradual microcrack closure with stress. Based on the chosen RPMs, four main facies were classified within the interval: low and high clay organic-rich shales, calcareous shales, and carbonates.

The organic-rich shales are differentiated based on clay content using the Vernik conventional shale model and characterized by high total porosity and total organic carbon (TOC). For RPM calibration, main minerals consist of clay (42% clay fraction for low clay and 70% for high clay), quartz, and calcite with a Reuss mixing method. Clay and grain parameters (such as GR, PEF, and CNL) were left open for the workflow to optimize and aid in petrophysical classification.

The calcareous shale facies were defined using the Vernik–Kachanov carbonate model, where grain parameters were defined as a mixture of calcite and clay and accounting for consolidated and unconsolidated phases of the rock framework along with porosity, cementation, and compaction effect. The carbonate facies consist of a mixture of calcite and quartz minerals with similar parameterization as calcareous shale facies, exhibiting low porosity, permeability, and usually treated as drilling hazards within the formation.

Once the prior facies proportions were specified, wells with associated elastic and petrophysical logs, working intervals, and pressure trends were combined to produce posterior models, model relevancy, and an RPM template of calibrated models. Figure 5 shows the predicted and measured log data across petrophysical, elastic, and pressure domains for one of the wells used in training. RPML facies prediction is validated against

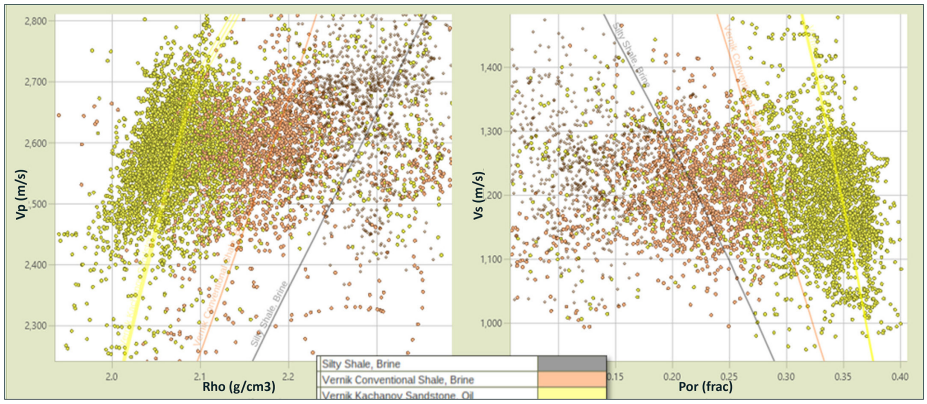

Figure 4. Parameterized RPMs generated from RPML plotted with well data. Theoretical trends include the Vernik and Kachanov sandstone model (yellow), Vernik conventional shale model (orange), and silty shale model (brown).

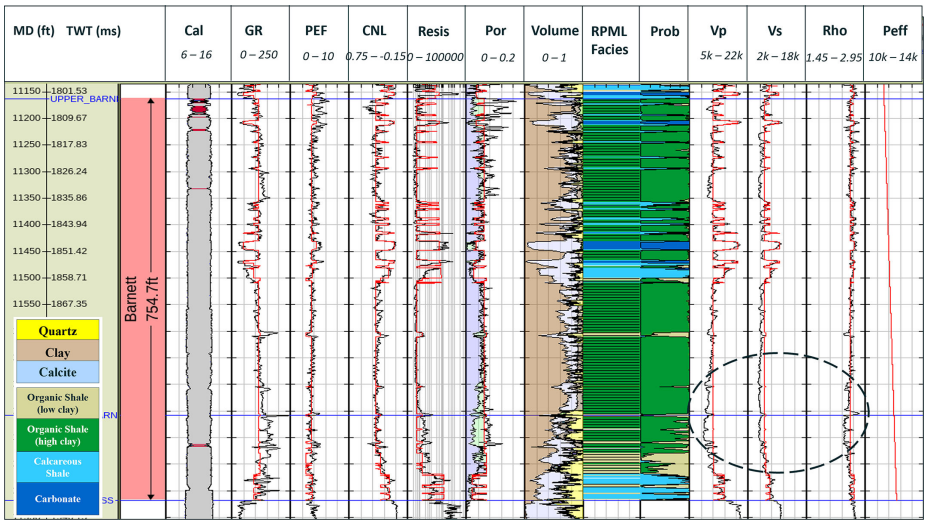

Figure 5. Predictions (red) versus measured log data (black) for one of the training wells along with facies classification in the Barnett interval. Low clay (< 42%) organic-rich shales with high TOC and porosity are predicted in lower Barnett, a particular facies of interest considered more ideal for fracture propagation.

petrophysics (volume track in Figure 5) to evaluate how the facies relate to mineralogy. Low clay zones (organic-rich shales) are characterized by high TOC, porosity, and clay fraction <42%. These facies are considered to be an additional source of hydrocarbon generation within the target and, in general, are more brittle (higher calcite and silica), making it more favorable for frac efficiency. It is also observed that the velocities are overpredicted in lower Barnett (black ellipse). This is a current limitation in the implementation of the Vernik conventional shale model, where kerogen is not included as a model parameter, thereby leading to overprediction in elastic properties in high TOC zones. We also observe low correlation between logs in upper Barnett, especially for total porosity where caliper becomes unstable, leading to spurious data measurement. In this case, RPML has corrected for tool anomaly and predicted properties within rock physics constraints. The close agreement between curves demonstrates the workflow's ability to reconstruct spurious logs while maintaining rock physics-consistent trends.

Further QC checks are generated to validate facies separation across different elastic and petrophysical domains (Figure 6) and ensure model relevancy. Low clay organic-rich shales exhibit higher resistivity (indicated in the Pickett plot) and relatively low K and Mu moduli (more siliceous), making these facies favorable for drilling targets. We also observe a separation between the low and high clay shales in the elastic domain (AI-V_P/V_S), indicating that one can resolve such facies with good quality seismic data. Plots such as these help validate the results not just from a rock physics perspective but also in petrophysical space, aligning interpretations across different disciplines and generating consistent facies and property predictions across wells.

RPML application and use case

Any subsurface workflow that relies on log prediction and facies classification can take advantage of this methodology. To validate the results of the training, the model was applied to a blind well (Figure 7) where only triple combo logs (GR, Resis, CNL, and Rho) were available as inputs. Results show the robustness of the model and how properties can be quickly estimated in data-scarce environments to assist with other quantitative interpretation workflows. One such application is well-to-seismic tie using forward-modeled V_P, V_S, and Rho predictions from RPML. Here, the workflow has predicted logs consistent with petrophysics and rock physics, enabling interpreters to achieve reliable seismic ties using only triple combo logs.

As previously shown, the workflow also provides per-facies depth trends, calibrated RPMs, and a final estimation of posterior-facies distribution (Figure 8). These proportions can be used as prior information for facies-based inversion and refined further for predicting facies in 3D using seismic data. Additional use cases include the development of robust low-frequency models to support seismic inversion workflows and the application of depth-varying Bayesian classification methods for improved facies prediction that accounts for changing burial and compaction trends.

Although the workflow produces strong correlations in the geologic settings presented, its performance still depends on the quality of the logs available. In addition, the model does not explicitly account for kerogen, which can lead to overestimation of elastic properties. Complex mineral mixtures are not explicitly represented and may need further refinement for future

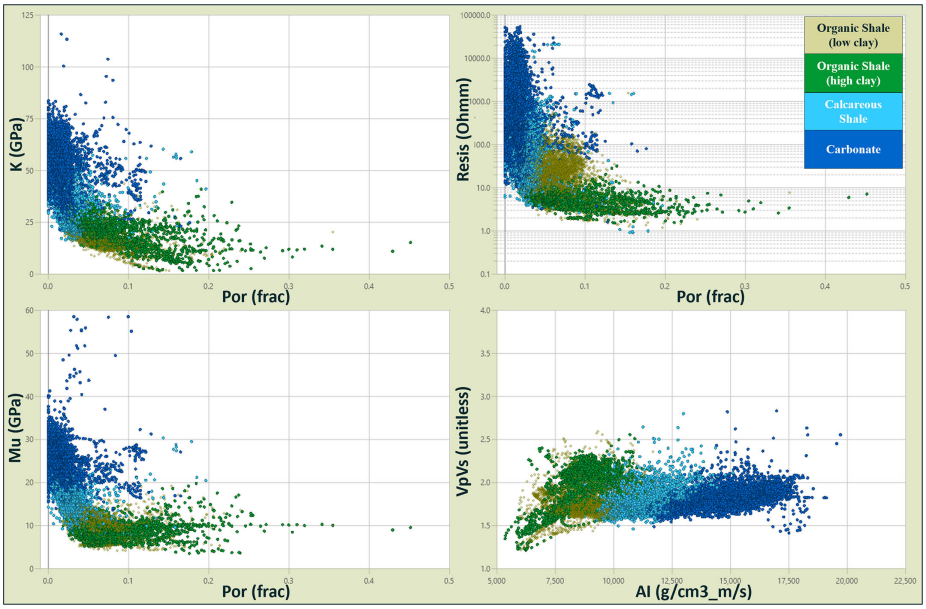

Figure 6. Multiwell matrix crossplot showing facies distribution within the Barnett interval in rock physics (K-Por, Mu-Por), petrophysics (Resis-Por), and elastic (AI-V_P/V_S) domains. Consistent alignment of facies distribution in different domains helps validate predictions and align interpretations.

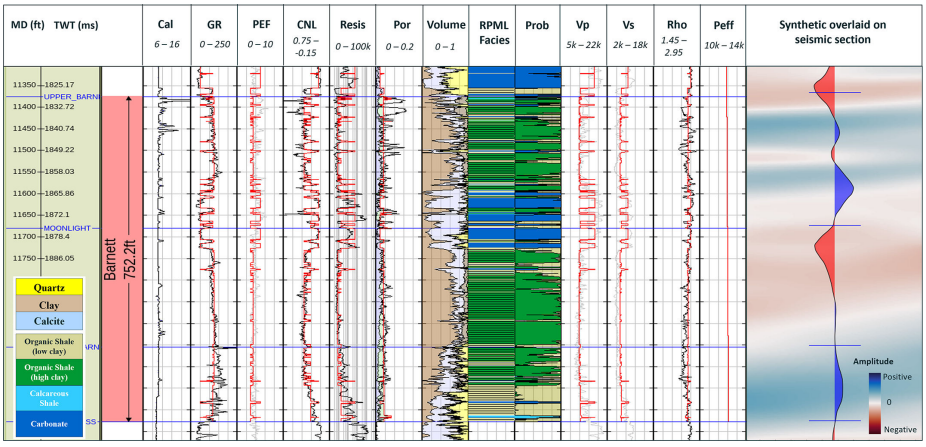

Figure 7. The RPML workflow is applied to a blind well to test the robustness of the model. In this case, V_P, V_S, Por, PEF, and Peff are predicted along with a facies classification. In situ logs (in black and gray) are displayed for property comparison. The predicted velocity shows strong agreement with the measured log, with a correlation coefficient of 82% for compressional velocity (V_P) and 88% for shear wave velocity (V_S). Also shown is a synthetic trace (generated using a statistical wavelet) overlaid on seismic for well-tie comparison.

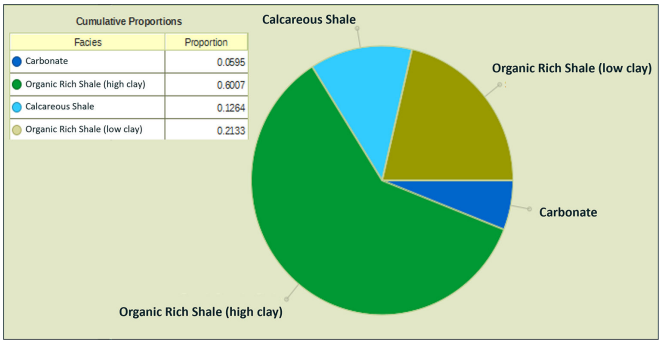

Figure 8. Posterior facies plot outputting cumulative facies proportions within the Barnett interval. Based on RPML prediction, the final facies distribution at one of the blind wells consists of 6% carbonates, 12.6% calcareous shales, 21.3% low clay, and 60.1% high clay organic-rich shales.

work. Finally, the workflow assumes a single pressure trend as input, which could be improved to better capture lateral pressure variations and anomalies. Nonetheless, rock physics-guided machine learning methodology produces robust property predictions constrained within physical bounds and significantly expands the number of wells available for reservoir characterization.

Conclusion

This study presents a rock physics-guided machine learning workflow for predicting reservoir properties across multiple zones and facies. By integrating rock physics models with statistical learning, the RPML approach provides physically consistent predictions of elastic and petrophysical properties while reducing the manual effort required for rock physics template calibration. Case studies from the Athabasca oil sands and the Midland Basin demonstrate the workflow's ability to reconstruct missing logs, estimate facies likelihoods, and calibrate rock physics relationships across multiple wells. Blind-well validation confirms that the method can generate reliable predictions in previously unseen wells. The RPML workflow provides a practical framework for integrating rock physics knowledge with data-driven analysis, supporting reservoir characterization and inversion-oriented modeling in complex multizone reservoirs. TLE

Acknowledgments

The authors would like to thank Athabasca Oil Corporation and Fasken Oil and Ranch for providing the data for this study and to our colleagues at Ikon Science for their technical input.

Data and materials availability

Data associated with this research are confidential and cannot be released.

Corresponding author: pbhatnagar@ikonscience.com

References

Anantharamu, V., P. Bhatnagar, and R. Bianco, 2024, Comparative study of advanced machine learning methods for reservoir property

prediction and optimizing production: 85th EAGE Annual Conference & Exhibition, https://doi.org/10.3997/2214-4609.2024101736.

Bhatnagar, P., V. Anantharamu, and R. Bianco, 2023, December 14, Understanding the depositional model of the Spraberry formation using facies inversion: Third International Meeting for Applied Geoscience & Energy, SEG/AAPG, 845–849, https://doi.org/10.1190/image2023-3910350.1.

Bhatnagar, P., S. Verma, and R. Bianco, 2019, Characterization of mass transport deposits using seismic attributes: Upper Leonard Formation, Permian Basin: Interpretation, **7**, no. 4, SK19–SK32, https://doi.org/10.1190/INT-2019-0036.1.

Bianco, R., P. Bhatnagar, and V. Anantharamu, 2024, Rock Physics Modeling in Unconventionals: A Midland Basin Case Study: The Unconventional Resources Technology Conference, https://doi.org/10.15530/urtec-2024-4038101.

Dempster, A. P., N. M. Laird, and D. B. Rubin, 1977, Maximum likelihood from incomplete data via the EM algorithm: Journal of the Royal Statistical Society Series B, **39**, no. 1, 1–22, https://doi.org/10.1111/j.2517-6161.1977.tb01600.x.

Leckie, D. A., and D. G. Smith, 1992, Early Cretaceous paleogeography of the Western Canada Sedimentary Basin: Geological Survey of Canada Bulletin, **436**, 1–37.

Lewis, A., T. Mackay, R. Dimit, B. Bracken, and A. Bell, 2024, A Case Study on the Emergence of the Barnett Shale in the Midland Basin, Ector County, Texas: The Unconventional Resources Technology Conference, 2364–2372, https://doi.org/10.15530/urtec-2024-4055274.

Liu, E., N. M. Miller, S. Every, A. J. Dale, E. L. Ferreira, A. Bazzell, J. A. Bryant, et al, 2025, Application of Machine Learning to 3D Geomechanical Modeling for Estimating Resource Accessibility in the Permian Basin, USA: ADIPEC, https://doi.org/10.2118/229572-MS.

Pandey, Y. N., A. Rastogi, S. Kainkaryam, S. Bhattacharya, and L. Saputelli, 2020, Machine Learning in the Oil and Gas Industry. Texas: Apress.

Pervukhina, M., G. Vasilenko, and T. Pervukhina, 2015, Anisotropic shale model for velocity and porosity predictions: Geophysics, **80**, no. 6, D303–D312.

Smith, S. D., 1994, Stratigraphy and sedimentology of the Mannville Group in northeastern Alberta: Geological Survey of Canada Bulletin, **469**, 65–82.

Smith, J., and R. Lee, 2021, Geological variability and its impact on SAGD recovery in the Athabasca Oil Sands: Journal of Petroleum Geology, **45**, no. 2, 123–136.

Suleymanov, V., A. El-Husseiny, G. Glatz, and J. Dvorkin, 2023, Rock physics and machine learning comparison: elastic properties prediction and scale dependency: Frontiers in Earth Science, **11**, 1095252, https://doi.org/10.3389/feart.2023.1095252.

Teitel, A., 2025, Beyond cut-offs: accelerating facies classification with RPML – A case study from the Athabasca Oil Sands, CSEG, https://cseg.ca/beyond-cut-offs-accelerating-facies-classification-with-rpml-a-case-study-from-athabasca-oil-sands, accessed 28 November 2025.

Verma, S., S. Bhattacharya, N. U. M. K. Chowdhury, and M. Tian, 2021, A new workflow for multi-well lithofacies interpretation integrating joint petrophysical inversion, unsupervised, and supervised machine learning: First International Meeting for Applied Geoscience & Energy, SEG/AAPG, Expanded Abstracts, https://doi.org/10.1190/segam2021-3584118.1.

Vernik, L., 2016, Seismic Petrophysics in Quantitative Interpretation: SEG, https://doi.org/10.1190/1.9781560803256.

Vernik, L., and M. Kachanov, 2010, Modeling elastic properties of siliciclastic rocks: Geophysics, **75**, no. 6, E171–E182, https://doi.org/10.1190/1.3494031.

Xu, S., and M. A. Payne, 2009, Modeling elastic properties in carbonate rocks: The Leading Edge, **28**, no. 1, 66–74, https://doi.org/10.1190/1.3064148.

Zhao, L., J. Liu, M. Xu, Z. Zhu, Y. Chen, and J. Geng, 2024, Rock-physics-guided machine learning for shear sonic log prediction: Geophysics, **89**, no. 1, D75–D87, https://doi.org/10.1190/geo2023-0152.1.

Zhu, Y., E. Liu, A. Martinez, M. A. Payne, and C. E. Harris, 2011, Understanding geophysical responses of shale-gas plays: The Leading Edge, **30**, no. 3, 332–338, https://doi.org/10.1190/1.3567265.